

SPECIAL PROJECT PROGRESS REPORT

Progress Reports should be 2 to 10 pages in length, depending on importance of the project. All the following mandatory information needs to be provided.

Reporting year 2018

Project Title: Go Beyond Current Limitations of Climate Simulation and Projection over Land

Computer Project Account: spitales

Principal Investigator(s): Alessandri Andrea

Affiliation: ENEA (Italy) (other affiliation: KNMI, Netherlands)

Name of ECMWF scientist(s) collaborating to the project (if applicable)

Start date of the project: 1 January 2016

Expected end date: 31 December 2018

Computer resources allocated/used for the current year and the previous one (if applicable)

Please answer for all project resources

		Previous year		Current year	
		Allocated	Used	Allocated	Used
High Performance Computing Facility	(units)	5 million	4499650 (90%)	5 million	659200 (13%)
Data storage capacity	(Gbytes)	50000	2403	50000	9106

Summary of project objectives

(10 lines max)

The objectives of this special project are (i) develop a process-based albedo parameterization in EC-Earth, (ii) validate and assess the effects of the new albedo scheme on the simulated climate during the last Century historical period and (iii) evaluate the interactions and feedbacks of the interactive albedo in the future climate projections (CMIP6).

The couplings and feedbacks of the newly introduced interactive albedo will be assessed together with the interactions with the changes of water availability (soil moisture and snow) as well as changes in land cover/land use types.

Summary of problems encountered (if any)

(20 lines max)

The finalization of the EC-Earth ESM to be used for CMIP6 runs has been delayed in the framework of the EC-Earth consortium due to problems encountered with new Earth System components and related physical parameterizations issues with the CMIP6 forcings and various technical problems within the code. Differently from the expected release by the end of 2017, at current stage the EC-Earth ESM for CMIP6 is not yet finalized and is therefore delaying the execution of the planned climate-projection simulations (GLACE A and GLACE B).

Summary of results of the current year (from July of previous year to June of current year)

This section should comprise 1 to 8 pages and can be replaced by a short summary plus an existing scientific report on the project

During the third reporting period of the project we finalized the development of a process-based albedo parameterization in EC-Earth. The goal is to replace the static albedo representation (currently used in IFS/HTESSSEL) with a time-varying parameterization as a function of effective vegetation cover and soil moisture. The initial objective of the parameterization is to reproduce as best as possible the currently-used MODIS (Morcrette et al., 2008) monthly climatology of total albedo (snow-free) that is currently prescribed to IFS/HTESSSEL as boundary condition, while also suitably modeling realistic seasonal and interannual variations. Therefore, the problem is to parameterize the albedo characteristics per type of vegetation (Aveg) and per type of soil (Asoil) using the available (i) global maps of satellite derived total snow-free albedo (Aobs) and/or (ii) obtain estimates from Field campaigns and field station measures.

HTESSSEL subgrid discretization:

HTESSSEL (Balsamo et al. 2009) discretization, for each grid point, solves for up to six different land surface tiles that may be present over land (bare ground, low and high vegetation, intercepted water by vegetation, and shaded and exposed snow). Surface radiative, latent heat and sensible heat fluxes are calculated as a weighted average of the values over each tile. The background tile fractions (bare ground, A_b , low and high vegetation maximum fractional coverages, $A_{l,h}$) are prescribed from a static land-use map ensuring that each grid point sum to unity:

$$1 = A_l \times C_l + A_h \times C_h + A_b \quad (1)$$

In (1), $C_{l,h}$ is the density of vegetation that is parameterized according to the Lambert Beer (LB) law of extinction of light under a vegetation canopy (included in EC-Earth starting from version 2.4, while tabled values were used before; Alessandri et al., 2017):

$$C_{l,h} = 1 - \exp(-0.5LAI_{l,h}) \quad (2)$$

And so the actual vegetation cover (hereinafter effective vegetation cover, C_{eff}):

$$Ceff_{l,h} = A_{l,h} [1 - \exp(-0.5LAI_{l,h})] \quad (3)$$

Given the HTESSEL discretization, it follows that total albedo in each grid-point can be represented as a weighted combination of low and high effective cover in each pixel plus a background soil albedo:

$$\begin{aligned} Atot(t) = & \\ & Aveg_{l,iveg} [iveg = TVL] * Ceff_l(t) + \\ & + Aveg_{h,iveg} [iveg = TVH] * Ceff_h(t) + \\ & + Asoil * [1 - Ceff_l(t) + Ceff_h(t)] \end{aligned} \quad (4)$$

where TVL and TVH are the dominant vegetation types for each grid point for low and high vegetation, respectively.

Methodologies employed to estimate Vegetation look-up table and soil albedo

Several methods have been tested and compared in order to parameterize the interactive behaviour of vegetation and soil albedo. To be able to describe/compare all methods using the same notation, we use the general formalism that can be associated to any estimation based on minimization of Norms $\| \cdot \|_p$ ($p=1,2,3,\dots$; also often indicated as L^p -Norms):

$$\|x\|_p = \left(\sum_i (x_i^p) \right)^{1/p}$$

All methods have been applied/compared on the native reduced gaussian grid used in IFS (standard resolution) and using area weighting according to the relative grid-point areas. The snow-free monthly MODIS albedos and LAI data are used in the same reduced gaussian grid as defined in the boundary conditions file for IFS (ICMCL file). On the other hand the independent GLCF albedo data (See Section 4 Results) had to be interpolated from regular $0.05^\circ \times 0.05^\circ$ longitude/latitude grid into the same reduced Gaussian grid for comparison. Similarly, the LAI3g leaf area index (LAI) data have been interpolated from original $0.5^\circ \times 0.5^\circ$ regular grid.

REGRESSION METHOD (REG)

Assumptions:

-HTESSEL subgrid discretization is assumed as representative of real world.

-Albedo soil map from Rechid et al. (2009) is assumed as perfect.

L^2 -Norm is used in the following regression:

$$\min \left\| \frac{A_{fig,iveg} - Atot_{obs} (1 - Ceff_{L,H}) * Asoil_{Rechid}}{Ceff_{L,H}} \right\|_2$$

ESTIMATE METHOD [EST]

Assumptions:

-HTESSEL subgrid discretization is assumed as representative of real world.

-A threshold for the effective vegetation cover ($Ceff_{l,h}$) is assumed as filter for the selection of grid points representative of each specific vegetation type.

Priority is given to the estimation of the vegetation look-up table parameters. Approach is conservative to avoid overfitting of the data and related error compensation.

In the following the minimization problem that has been used:

$$\min \left\| A_{ext,iveg} - Atot_{obs} \right\|_2 \quad \text{only for } Ceff_{l,h} > \max_threshold_iveg \text{ and } TVL \text{ or } TVH = iveg$$

where $\max_threshold_iveg$ for $Ceff_{iveg}$ is the result of an iterative selection procedure, for each vegetation type, that tries to get by one hand the maximum threshold possible while, on the other hand, ensuring a large and robust sample for the estimate (convergence of estimates and Gaussian behaviour of the sample frequency distribution). Note that $Ceff$ is the effective (meaning actual) vegetation cover and not $A_{l,h}$ i.e. the max theoretical vegetation cover (meaning the area not

occupied by other type of cover, i.e. lakes, land ice). The threshold is chosen [arbitrarily] with the objective to obtain large enough sample of data so that the samples are as much as possible representative of a population with random and independent sampling errors in the estimates. Solution of this minimization problem is simply the average of the sample for each vegetation type. Associated to each vegetation-type estimate, we can obtain the uncertainty bounds using the percentiles in the corresponding normal distribution of the sample.

ESTIMATE + ESTIMATE-new-MAP METHOD [EST+newmap]

Same as ESTIMATE method but assuming that the vegetation albedo look-up table provided by ESTIMATE is perfect estimate.

The above assumption allows to solve for an additional minimization problem for a soil albedo map $A_{soil,ext}$ that is consistent with the look-up table values computed using ESTIMATE:

$$\min || Atot_{obs}(i,j,t) - Aveg_{ext,iveg=TVL(i,j)} * Ceff_L(i,j,t) - Aveg_{ext,iveg=TVH(i,j)} * Ceff_H(i,j,t) - A_{soil,ext}(i,j) [1 - Ceff_L(i,j,t) - Ceff_H(i,j,t)] ||_1$$

The soil albedo maps (hereinafter ESTIMATE-new-MAP) have been estimated for the two spectral bands and the two components (parallel and diffuse). Minimum and maximum acceptable values of observable soil albedos were obtained from available atlases from geographers/pedologists (e.g. Dickinson et al., 1993, Hartmann et al. 1994). For each grid point we checked that the obtained soil albedo values stay within the observable range and corrected the values accordingly when necessary.

Soil Look-up Table Method [SLT]

A soil look-up table is estimated following a similar method than for the look-up table of vegetation (ESTIMATE). The objective is to estimate a specific albedo of soil ($A_{soil_{isoil}}$) to each of seven soil categories defined in HTESSSEL based on different textures: Coarse, Medium, Medium-fine, Fine, very fine, organic, tropical organic.

Assumptions:

-HTESSSEL subgrid discretization is assumed as representative of real world.

-A max threshold for the effective vegetation cover ($Ceff_{tot}$) is assumed as filter for the selection of grid points representative of each specific soil types.

-Deserts are excluded by selecting only those points where vegetation is theoretically possible and so where structured soil is in place (in contrast with deserts where soils are not present), that is where $A_{l,h}$ (i.e. the max theoretical vegetation cover) is large enough, i.e. $CVL+CVH>0.5$.

The soil albedo look-up table values have been estimated for the two spectral bands and the two components (parallel and diffuse) by selecting the grid points where the total effective vegetation cover is small enough, and such that the measures can be attributed to points dominated by one of possible soil types (soil_type=isoil; no coexistence of more than one soil-type is possible in HTESSSEL):

$$(Cveff_{tot}) < threshold_{soil}$$

where $Cveff_{tot}$ is the total effective vegetation cover for high and for low vegetation

$$\min || A_{slt,isoil} - Atot_{obs} ||_2 \quad \text{only for } Ceff_l + Ceff_h < \min_threshold \text{ and for each soil_type=isoil}$$

Experiments

The performance of the different albedo parameterizations has been analyzed on a set of historical simulations with AMIP-type (using HadISST SST and sea ice [Rayner et al. 2003] from the CMIP6 forcing dataset input4MIPs) setup spanning 28 years (1982-2009) with the latest available version (v3.2) of EC-Earth (see Table 1 for a summary of experiments performed). Three members have

been performed for each experiment. In all simulations, the vegetation LAI variability is prescribed from the LAI3g dataset based on the third generation GIMMS and MODIS satellite observations (Zhu et al., 2013). The model version used for all the experiments also include the enhanced vegetation sensitivity described in Alessandri et al. (2017). In the MODIS experiments the albedo is prescribed from satellite-derived MODIS monthly climatology (Morcrette et al. 2008) as in the current version of IFS/HTESSEL.

Experiment name	Albedo parameterization
MODIS	Climatological snow-free albedo from MODIS
EST+SLT	Vegetation albedo from EST, soil albedo from SLT
REG+Rechid	Vegetation albedo from REG, soil albedo from Rechid map
EST+newmap	Vegetation albedo from EST, new soil albedo map

Table 1. Summary of AMIP experiments performed with EC-Earth v3.2. Period: 1982-2009, three members, LAI prescribed from LAI3g observations.

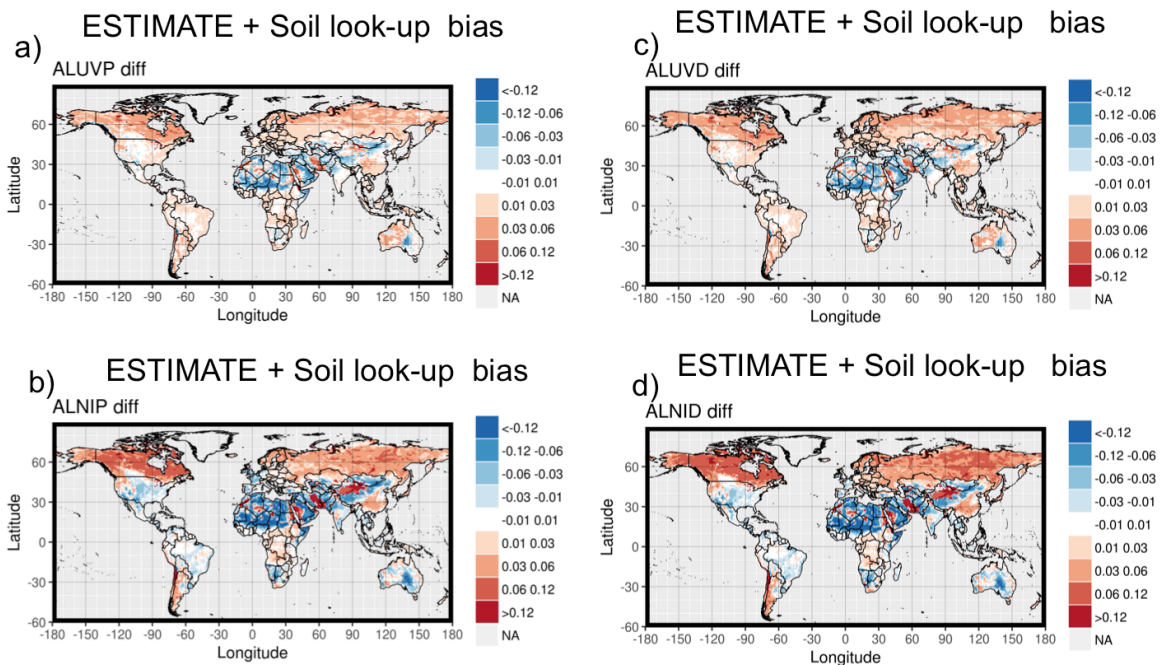


Figure 1: ESTIMATE+Soil look-up table bias: Annual average of difference between simulated and MODIS albedo in the different spectral bands in the ESTIMATE+Soil look-up table case (ALUVP=visible, direct; ALUVD=visible, diffuse; ALNIP=near infrared, direct; ALNID=near infrared, diffuse).

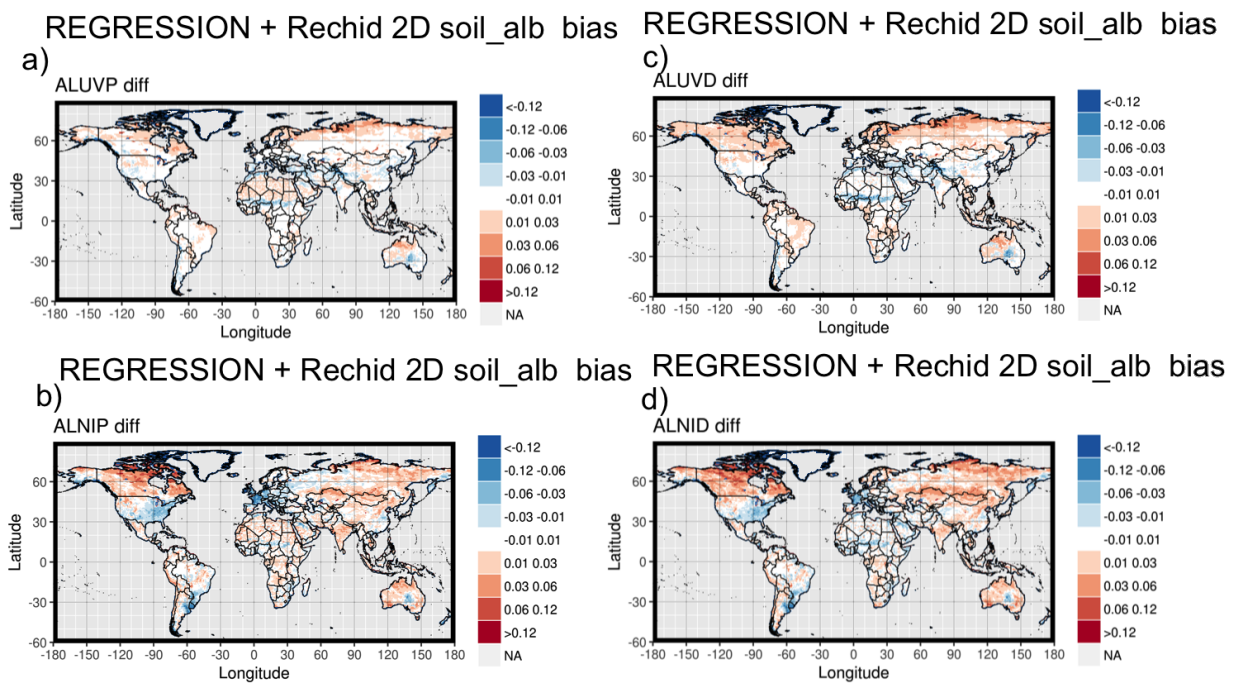


Figure 2: Same as Figure 1 but for REGRESSION + Rechid 2D soil albedo map. Fixed soil albedo map from Rechid et al. (2009).

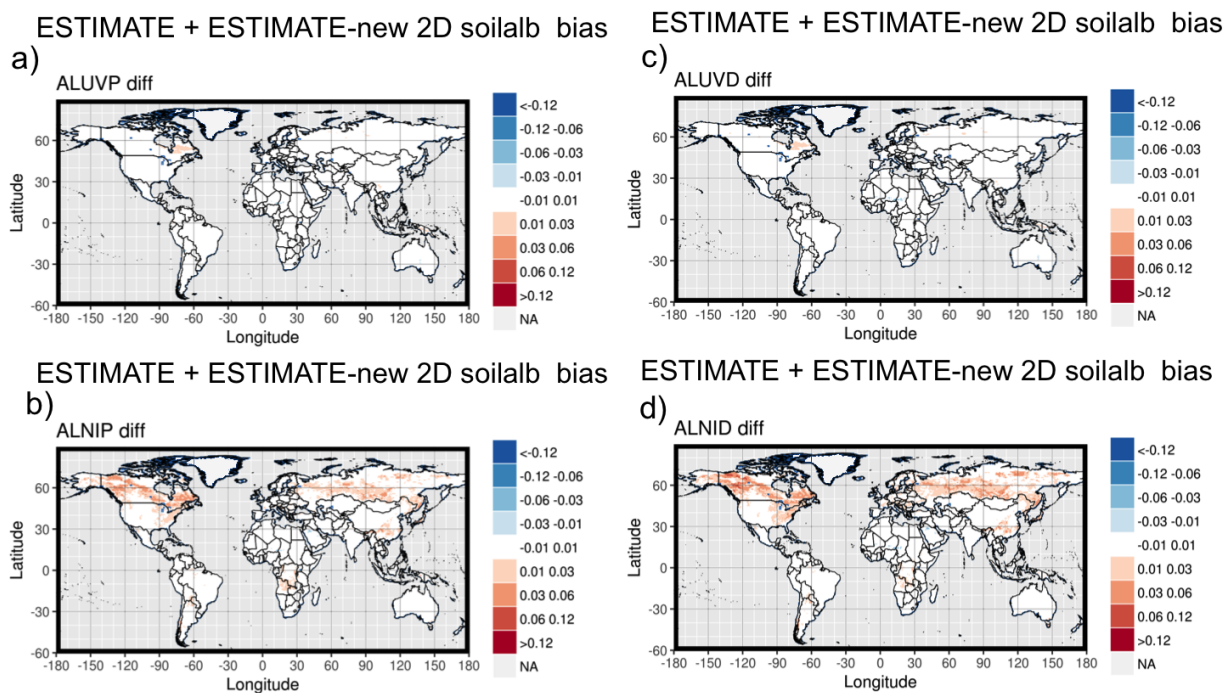


Figure 3: Same as Figure 1 but for ESTIMATE + ESTIMATE-new 2D soil albedo map

BIAS (RMSE)	ANN	JJA	DJF
ESTIMATE + Soil look-up table	0.05 (0.31)	0.01 (0.27)	0.05 (0.44)
REGRESSION + Rechid 2D soil_alb	-0.02 (0.16)	0.03 (0.44)	-0.03 (0.37)
ESTIMATE + ESTIMATE-new 2D soil_alb	0.00 (0.15)	0.01 (0.27)	0.01 (0.29)

Table 2. Global mean bias (and RMSE in brackets) of 2m-temperature with respect to control simulation with prescribed MODIS

Compared to REG+Rechid and EST+newmap, that use 2D gridded estimates of the background soil albedo, the method employing the soil look-up table (Figure 1) introduces a discretization of the representation in soil classes that reduces the performance in reproducing the MODIS albedo. The associated 2m-temperature biases and RMSE tend to be compensated on a global average. The use of a fixed soil albedo map produces significantly better results, except for June-July-August (JJA).

Implementation of the soil albedo dependence on soil moisture

The results presented above indicate a strong sensitivity to the modeled soil albedo. This motivated us to move forward towards a process-based parameterization of soil albedo that can account for the dependence upon soil moisture (SM). The dependence of soil albedo on SM has been investigated by using the latest released global observational datasets of albedo from COPERNICUS global land service (<https://land.copernicus.eu/global/>) for the period 1999-2016. The dataset provides parallel and diffuse albedo for both visible and near-infrared bands, as required by EC-Earth/IFS. In order to produce a snow-free albedo dataset from COPERNICUS data we used the snow extent dataset from NOAA (Brown and Robinson 2011) and filtered out all albedo points where snow is present in the timeseries. More than 50% of the grid-points of the global albedo land-domain (space-time) is marked as snow-free and used in the analysis. Soil moisture is based on the latest ESA product (Dorigo et al. 2017) while for the computation of effective vegetation covers we used the LAI observational leaf area index dataset from COPERNICUS (see eq. 2). The above datasets have been used in the overlapping period 1999-2016, that is available for all the observational products.

To disentangle the soil albedo component ($A_{soil}[t]$) from the observed total albedo, a linear decomposition can be performed (see eq. 4) using the vegetation-albedo maps from Otto et al. (2011) as follows:

$$A_{soil}[t] = (A_{tot}[t] - A_{veg} * C_{eff}[t]) / (1 - C_{eff}[t])$$

Furthermore, points with $C_{eff} > 0.8$ are discarded from subsequent analysis.

The link between A_{soil} and SM depends mainly on two soil properties: (i) texture and (ii) color. Soil color map from Dickinson et al. (1993) considers 9 soil colors, from light (1) to dark (8) and one additional class (9) for deserts. HTESSEL soil texture map considers 7 soil types: coarse, medium, medium-fine, fine, very-fine, organic, tropical-organic. By combining soil color and texture information we divided the land areas into $9*7=63$ soil classes. For each soil class (texture and color) we seek a robust (statistically significant) linear relation between albedo and soil moisture for the four albedo components:

$$A_{soil}(i,j,t) = a_{tex,col} * SM(i,j,t) + b_{tex,col}$$

Figure 4 shows the linear relation between the visible component of A_{soil} and SM, together with the linear regression considering all land points. It is clear from the figure how the scatterplot cloud tends to be clustered in the different color classes. A similar clustering exist with respect to the

different soil textures (not shown). As an example, Fig. 5 shows the medium-fine/colour 4 soil class with its statistically significant (1% significance level) linear relation well represented.

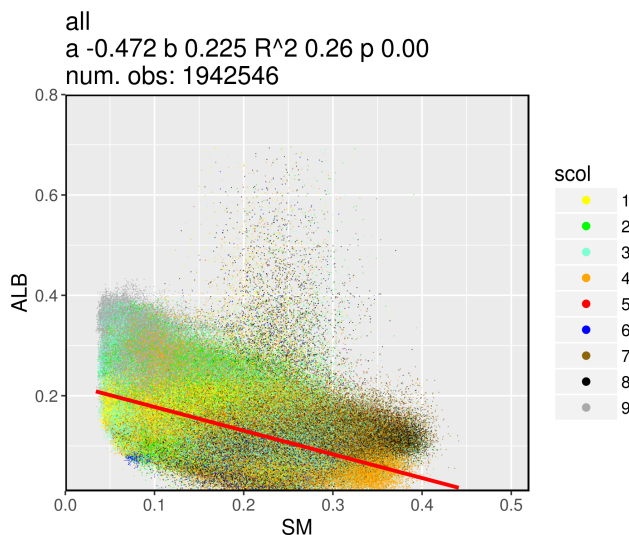


Figure 4: Scatterplot of the visible component of Asoil vs Soil Moisture, together with the linear regression considering all land points. Different colors stand for the 9 soil colors considered in the soil color map by Dickinson et al (1993).

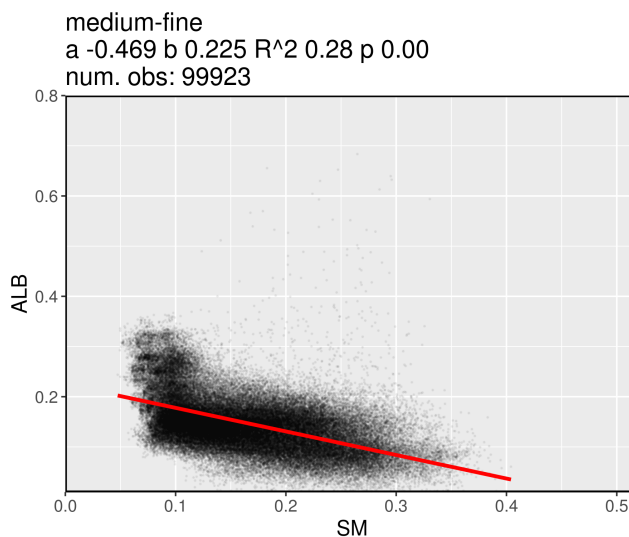


Figure 5: Scatterplot the of the visible component of Asoil vs Soil Moisture for the medium-fine/colour 4 soil class with its statistically significant (1% significance level) linear relation.

CMIP6-LS3MIP setup

Two sets of forced experiments will be carried out where land surface states are prescribed from an a priori defined database (GLACE-A and GLACE-B), which is the contribution to the proposed activities in the framework of the Land Surface, Snow, and Soil moisture MIP (LS3MIP; <http://www.climate-cryosphere.org/activities/targeted/ls3mip>) that is sponsored by the WCPR's CMIP6, GEWEX and the CliC project.

In collaboration with colleagues from Lund University we are therefore preparing the technical interface to prescribe land-surface states in HTESSEL-IFS for the experiments following the LS3MIP protocol, which requires to prescribe land surface states at daily frequency. It is required reading external files daily and replacing land surface variables throughout the entire simulations. A nudging procedure for soil moisture content has been developed and implemented in a dedicated 'ls3mip' branch in the development portal of the EC-Earth ESM model.

References

- Alessandri A., Catalano F., De Felice M., van den Hurk B., Doblas-Reyes F., Boussetta S., Balsamo G., Miller P. A., 2017: Multi-scale enhancement of climate prediction over land by increasing the model sensitivity to vegetation variability in EC-Earth. *Clim. Dyn.*, 49, 1215-1237, doi:10.1007/s00382-016-3372-4
- Balsamo, G., A. Beljaars, K. Scipal, P. Viterbo, B. van den Hurk, M. Hirschi, and A. K. Betts, 2009: A revised hydrology for the ECMWF model: Verification from field site to terrestrial water storage and impact in the integrated forecast system. *J. Hydrometeor.*, 10, 623–643, doi:10.1175/2008JHM1068.1.
- Brown, R. D. and Robinson, D. A.: Northern Hemisphere spring snow cover variability and change over 1922–2010 including an assessment of uncertainty, *The Cryosphere*, 5, 219-229, <https://doi.org/10.5194/tc-5-219-2011>, 2011
- Dickinson, R. E., A. Henderson-Sellers, and P. J. Kennedy, 1993: *Biosphere-atmosphere Transfer Scheme (BATS) Version 1e as Coupled to the NCAR Community Climate Model*. NCAR Technical Note NCAR/TN-387+STR, doi:10.5065/D67W6959
- Dorigo, W., et al., 2017: ESA CCI Soil Moisture for improved Earth system understanding: State-of-the art and future directions, *Remote Sensing of Environment*, 203, 185-215, doi:10.1016/j.rse.2017.07.001
- Hartman, D.L., 1994: *Global Physical Climatology*, International Geophysics Series, Ed. R. Dmowska and J.R. Holton, Academic Press, Vol. 56, 411 pp.
- Morcrette, J.-J., Barker, H. W., Cole, J. N. S., Iacono, M. J., Pincus, R., 2008: Impact of a New Radiation Package, McRad, in the ECMWF Integrated Forecasting System. *Mon. Wea. Rev.*, 136, 4773-4798.
- Otto, J., T. Raddatz, and M. Claussen, 2011: Strength of forest-albedo feedback in mid-Holocene climate simulations, *Clim. Past*, 7, 1027-1039, doi:10.5194/cp-7-1027-2011
- Rayner, N. A.; Parker, D. E.; Horton, E. B.; Folland, C. K.; Alexander, L. V.; Rowell, D. P.; Kent, E. C.; Kaplan, A. (2003) Global analyses of sea surface temperature, sea ice, and night marine air temperature since the late nineteenth century *J. Geophys. Res.* Vol. 108, No. D14, 4407 10.1029/2002JD002670
- Rechid, D., T. J. Raddatz, and D. Jacob, 2009: Parameterization of snow-free land surface albedo as a function of vegetation phenology based on MODIS data and applied in climate modelling, *Theor. Appl. Climatol.*, 95, 245-255, doi:10.1007/s00704-008-0003-y
- Zhu, Z., Bi, J., Pan, Y., Ganguly, S., Anav, A., Xu, L., Samanta, A., Piao, S., Nemani, R. R., and Myneni, R. B., 2013: Global Data Sets of Vegetation Leaf Area Index (LAI)3g and Fraction of Photosynthetically Active Radiation (FPAR)3g Derived from Global Inventory Modeling and Mapping Studies (GIMMS) Normalized Difference Vegetation Index (NDVI3g) for the Period 1981 to 2011, *Remote Sens.*, 5, 927–948.

List of publications/reports from the project with complete references

- Alessandri A., Catalano F., De Felice M., van den Hurk B., Doblas-Reyes F., Boussetta S., Balsamo G., Miller P. A., 2017: Multi-scale enhancement of climate prediction over land by increasing the model sensitivity to vegetation variability in EC-Earth. *Clim. Dyn.*, 49, 1215-1237, doi:10.1007/s00382-016-3372-4
- van den Hurk, B., Kim, H., Krinner, G., Seneviratne, S. I., Derksen, C., Oki, T., Douville, H., Colin, J., Ducharne, A., Cheruy, F., Viovy, N., Puma, M. J., Wada, Y., Li, W., Jia, B., Alessandri, A., Lawrence, D. M., Weedon, G. P., Ellis, R., Hagemann, S., Mao, J., Flanner, M. G., Zampieri, M., Materia, S., Law, R. M., and Sheffield, J., 2016: LS3MIP (v1.0) contribution to CMIP6: the Land Surface, Snow and Soil moisture Model Intercomparison Project – aims, setup and expected outcome, *Geosci. Model Dev.*, 9, 2809-2832, doi:10.5194/gmd-9-2809-2016.

Summary of plans for the continuation of the project

(10 lines max)

The enhanced EC-Earth model, including the newly developed process-based albedo parameterization, will be used to evaluate the interactions and feedbacks of the albedo for the last century historical period and in the future climate projections (CMIP6). The couplings and feedbacks of the new process-based albedo parameterization will be analyzed together with the interactions with the changes of water availability and the changes in land cover/land use types.

The finalization of the EC-Earth ESM, in the framework of the EC-Earth consortium, to be used for CMIP6 has been delayed due to several problems encountered with new Earth System components and issues with the CMIP6 forcings and various technical problems within the code. This is going to also delay the execution of the planned climate-projection simulations (GLACE A and GLACE B) and could affect the timely completion of the simulations that are planned during 2018.